CONTROL OF DUAL-MODE DYNAMICS FOR NANOMETER POSITIONING OF BALL SCREW

Sohair F. Rezeka
Department of Mechanical Engineering, Faculty of Engineering,
Alexandria University, Alexandria, Egypt.

ABSTRACT

In this paper, the adaptive feedforward control is proposed to improve the nanometer positioning accuracy of ball screws. The control system consists of an adaptive disturbance compensator, an adaptive feedforward controller for the desired action, and a PI feedback controller using the position error as a driving signal. The nonlinear characteristics of the friction mechanism is represented by the reset integrator model. This model simulates both the microdynamic and the macrodynamic modes. The stability of the adaptive law was established based on Popov's theorem. The performance of the suggested control technique was investigated in tracking different desired outputs and when a poor microdynamic model was employed. The resulting closed-loop responses were compared to those obtained while the ball screw motion was under PI control and non-adaptive feedforward control. Simulation results demonstrate the effectiveness and the robustness of the adaptive feedforward control, which produces better performance, and more consistent and predictable behavior than the other two controllers. The proposed control scheme does not require continuous tuning of the PI controller to get full advantage of the control.

Keywords: Precision control, Dual-mode dynamics.

INTRODUCTION

The increasing demands for better precision positioning systems have prompted an investigation into the nanometer positioning capabilities of ball screws. Although ball screws have been used for many years, they traditionally were not applied to problems requiring sub-micrometer accuracy.

Friction is the nemesis of precision control. It is responsible for many problems associated with the control and accuracy of ball screw. It can, for example, cause the moving body to "jitter" during the motion in any direction; it can cause large tracking errors when changing direction; and it may result in limit cycling about a final position. Open loop testing [1] indicated that small angle of rotation of ball screw (and subsequent slide displacement) occurs for any applied torque. Cuttino et al. [2] showed that the "spring" behavior, resulting from elastic deformation of the contact patches on the ball, allows for nanometer motion by the application of low torque. The study also revealed that the dynamics of the ball screw is characterized by two modes: the pre-breakaway dynamics (microdynamics) which are dominated by the observed elastic behavior, and the post-breakaway dynamics (macrodynamics) which are based on a classical dynamic friction model. Futami et al. [3] observed similar elastic pre-breakaway behavior in a ball bearing slide during nanometer motion.

Various position control techniques have been presented to deal with the stick-slip behavior [4-7]. However, these investigations were centered around the behavior of the ball screw at the nanometer level, and elastic deformation of friction contacts in the ball nut allow for nanometer motion without including a friction breakaway. Recently, Hubbel et al. [8] adopted a model reference adaptive control strategy for the microdynamics motion of the ball screw. They used a Lyapunov technique to derive adaptive laws which relied on both position and velocity errors. The scheme resulted in more predictable and consistent closed-loop responses than the PI scheme. However, during the application of the control strategy there were four arbitrary positive constants to be chosen to ensure the

convergence to the model. On the other hand, since the velocity was too low to be measured, it was calculated from the derivative of the position signal and consequently the system was sensitive to sensor noise.

Feedforward control is effective in tracking the time varying desired output signal, but it is sensitive to modelling error [9]. To increase the system robustness, an adaptive feedforward control was proposed by Tomizuka et al. [10]. The controller was evaluated using a good and poor model of a manipulator's link [11] and the results demonstrated the effectiveness of the approach. However, the literature review reveals that the adaptive feedforward control was not applied to precision positioning control.

In this paper, the dual-mode dynamics of the ball screw were modelled. The adaptive feedforward control approach was applied and the control strategy was based on the position error only. The stability of the closed-loop was investigated. The nanometer motion of the ball screw prior and post friction breakaway upon implementing PI position control, PI plus feedforward control, and PI plus adaptive feedforward control were compared.

FRICTION MODEL

The modelling of friction mechanism has been and continues to be a non-trivial task. Idealized Coulomb friction is a double-valued function at zero relative speed between the two connecting surfaces. When the external forces exceed the peak stiction force, the body will begin to slide, and the friction force at nonzero velocities will be less than the peak stiction force. Since the discontinuity at the origin is physically unrealistic and unacceptable for purposes of simulation, the "classical (Coulomb) friction model" approximates the discontinuity by a linear function with a steep slope around zero relative velocity. However, this technique can result in artificial simulation problems/errors such as limit cycle, position creep, and long computational times. Karnopp [12] developed an alternative approach to overcome the lack of verisimilitude of the classical model at low velocities. When the relative velocity is within a small band $\pm D_v$ the system "sticks", and while sticking the friction force exactly cancels the driving force. When the driving force exceeds the peak stiction force, the body accelerates and the model will switch from stick to slip mode. The Karnopp approach is difficult to incorporate into a simulation model because it requires the derivation of separate sets of equations for each possible slipping and sticking condition and the combination of these equations in a block diagram model in such a way that only one set is active at any time. Dahl model [13] relates the friction force to the relative velocity through measured parameters that determine the model effective spring rate and the peak sliding friction level. The model does not generate a stiction force that exceeds sliding force, and exhibits graceful transitions between the near-zero velocity and normal motion conditions. However, small artificial oscillations are present in the zero velocity region and may give inaccurate results for some configurations. Recently, Haessig et al. [14] introduced two new models: the bristle model and the reset integrator model. In the bristle model, the friction between the two surfaces is assumed to be caused by a large number of bristles (representing, for example, the molecular bonds) each contributing a small portion to the total friction force. The load contributed by each bristle is assumed to be proportional to the strain of the bristle and so the friction force is a function of position. When the strain of any particular bristle exceeds a certain level the bond is broken and a new bond having smaller strain is established. The friction load is made a function of velocity by varying the number of bristles. Because of the complexity experienced in applying the model and the associated long processing time, the bristle model is normally used only for simulation requiring extremely high fidelity. The reset integrator model was developed to reduce the computer time requirements of the bristle model while retaining its capacity to accurately represent slip-stick friction phenomenon. As shown in Figure (1), the input to the reset integrator model is the relative velocity between the contacting surfaces, v_r. The input to the integrator is determined as follows:

$$\dot{p}=0 \qquad \begin{array}{ll} v_r > 0 \ , & p \geq p_o \\ v_r < 0 \ , & p \leq -p_o \end{array}$$

otherwise,

$$\dot{p} = v_r \qquad (1)$$

p_o is the maximum amount of motion during sticking.

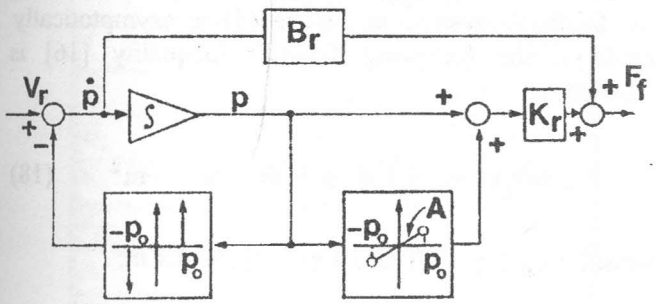

Figure 1. Reset integrator friction model.

When the system is in the stick mode (microdynamics), the friction force is determined by:

$$F_f = K_r p(1 + A) + B_r \dot{p} \qquad (2)$$

The first term shows that the stiction load is a function of position p and K_r is the spring rate. The stiction gradient A is added to generate the large loads that can occur during stiction. The damping term is added to eliminate the undamped oscillations that occur after the system has entered into a sticking mode. When slipping occurs, (macrodynamics), the integrator output is constant and is equal to p_o. The friction force is then given by:

$$F_f = K_r p_o \, \mathrm{sgn}(p_o) \qquad (3)$$

Hughes [15] showed that the reset integrator model is more versatile and accurate than both the Karnopp and Dahl models.

SYSTEM MODEL

The main components of the systems are: motor, ball screw, ball screw nut, and bearings. Considering the reset integrator model to represent the friction mechanism in the ball screw and the nut, the dynamics of the system are described in the microdynamic mode by:

$$J\ddot{\theta} + (B_r + B)\dot{\theta} + K_r(1 + A)\theta = u, \quad \theta \le \theta_o \qquad (4)$$

and in the macrodynamic mode the system equation is given by:

$$J\ddot{\theta} + B\dot{\theta} + K_r\theta_o = u, \quad \theta > \theta_o \qquad (5)$$

where J is the rotational inertia of the motor armature and the ball screw, B is the damping coefficient of the motor and the bearings, B_r, and K_r are the microdynamic damping coefficient and spring rate, respectively, A is the stiction gradient, θ_o is the maximum angle of rotation during stiction and u is the system input torque.

CONTROL STRATEGY

The microdynamic model of the plant includes three parameters (K_r, θ_o, and B_r) that are critical to the controller design. These parameters are not precisely known and may be time-varying. The objective of the controller design is to provide a predictable linear closed loop response and to track the desired nanometer motion regardless of uncertain plant parameters. Considering the adaptive feedforward control scheme shown in Figure (2), the input to the motor is

$$u = K_c\, e + \frac{1}{\tau}\int e\, dt + u_f(t) \qquad (6)$$

where

$$e = \theta_d - \theta$$

K_c and τ are a fixed gain and the integral time, respectively, of the PI controller. u_f is the feedforward control input and it is defined by:

$$u_f(t) = \hat{w}_o\theta_d + \hat{w}_1\dot{\theta}_d + \hat{w}_2\ddot{\theta}_d + \hat{w}_3\, v_c \qquad (7)$$

where θ_d (the desired output), $\dot{\theta}_d \wedge \ddot{\theta}_d$ and θ_d are bounded. The first three terms represent the feedforward control action for the desired output. The fourth term represents the adaptive compensator for the disturbance d, and v_c is constant.
By defining

$$\hat{\psi}^T(t) = [\hat{w}_o \;\; \hat{w}_1 \;\; \hat{w}_2 \;\; \hat{w}_3] \qquad (8)$$

and

$$\hat{\phi}^T(t) = [\theta_d \;\; \dot{\theta}_d \;\; \ddot{\theta}_d \;\; v_c] \qquad (9)$$

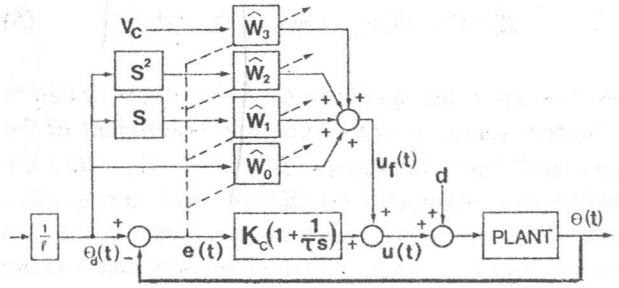

Figure 2. Adaptive feedforward control system.

$\hat{w}_i(t)$'s are adjusted by the following adaptive law:

$$d\hat{\psi} / dt = \gamma \quad \phi(t) \quad e(t) \qquad (10)$$

where γ is a positive adaptive gain.

Stability of the Adaptive Control Law

Equations (4) and (5) can be put in a general form as:

$$a\,\ddot{\theta} + b\,\dot{\theta} + c\,\theta = u + d \qquad (11)$$

Substituting Eqns (6) and (7) into Eq. (11) results in,

$$\ddot{\theta}_d(a-\hat{w}_2) + \dot{\theta}_d(b-\hat{w}_1) + \theta_d(c-\hat{w}_o) + v_c(-d/v_c-\hat{w}_3) = a\,\ddot{e} + b\,\dot{e} + (c+K_c)\,e + \frac{1}{\tau}\int e\,dt \qquad (12)$$

By defining

$$G(s) = \frac{s}{as^3 + bs^2 + (c+K_c)s + 1/\tau} \qquad (13)$$

$$\psi^T = [\; c \quad b \quad a \quad -d/v_c \;] \qquad (14)$$

$$\hat{\psi}^T = [\; \hat{w}_o - c\;\hat{w}_1 - b\;\hat{w}_2 - a\;\hat{w}_3 + d/v_c \;] \qquad (15)$$

where

$$\tilde{\psi}(t) = \hat{\psi} - \psi \qquad (16)$$

then Eq. (11) can be rewritten as:

$$e(t) = G(s)\,[\; -\tilde{\psi}^T(t)\,\phi(t)\;] \qquad (17)$$

Equation (17) describes the adaptation error dynamic and can be represented in an equivalent feedback form as in Figure (3). $\Phi(t)$ is bounded because $\theta_d, \dot{\theta}_d, \ddot{\theta}_t$ and v_c are bounded. G(s) is strictly positive real. Therefore, the feedback system in Figure (3) is asymptotically stable if the following Popov's inequality [16] is satisfied.

$$\eta(t_1) = \int_0^{t_1} \tilde{\psi}\;\phi\;e\;dt \;\geq\; -m^2 \qquad (18)$$

Substituting Eq. (10) into Eq. (18) results in:

$$\eta(t_1) = \int_0^{t_1} \tilde{\psi}\;(1/\gamma^T)\;(d\tilde{\psi}/dt)\;dt$$

Integrating by parts gives

$$\eta(t_1) = \frac{1}{2\gamma}\,[\;\tilde{\psi}^T(t_1)\;\tilde{\psi}(t_1) - \tilde{\psi}^T(0)\;\tilde{\psi}(0)]$$

$$\geq -\frac{1}{2\gamma}\;\tilde{\psi}^T(0)\;\tilde{\psi}(0)$$

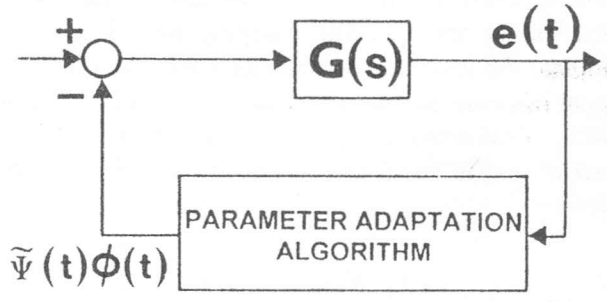

Figure 3. Feedback representation of error signal.

which verifies Popov's inequality. Therefore, the overall adaptive system is stable and the tracking error will converge to zero asymptotically. It should be noticed that when e(t) =0 , the motor is purely under feedforward control.

DISCUSSION OF RESULTS

Computer simulation of the ball screw system was performed under three controller configurations; proportional integral (PI), and PI plus either adaptive or non-adaptive feedforward control. The model parameters used in the calculations are listed in Table (1). The responses of the plant were examined during the tracking of two desired nut trajectories with maximum displacement of 25 nm and 400 nm.

Table 1. Model Parameters.

J	$2.5 * 10^{-4}$ kg.m^2
B	0.1 N.m.s/rad
B_r	14.5 N.m.s/rad
K_r	$1.6 * 10^6$ N.m/rad
θ_o	0.1 μ rad
A	0.05
Ball screw lead, l	1 mm/rad

1. **Performance with PI control:** The gain of the controller was adjusted to provide a slightly overdamped response to a 25 nm maximum displacement command. The result was compared to the desired displacement trajectory in Figure (4). The response is slow and the rise time is 3 seconds. However, when the same controller gain was used to achieve a 400 nm maximum nut-displacement, the closed-loop response varies significantly and it is unacceptable. The controller gain is tuned on to result in the response shown in Figure (5).

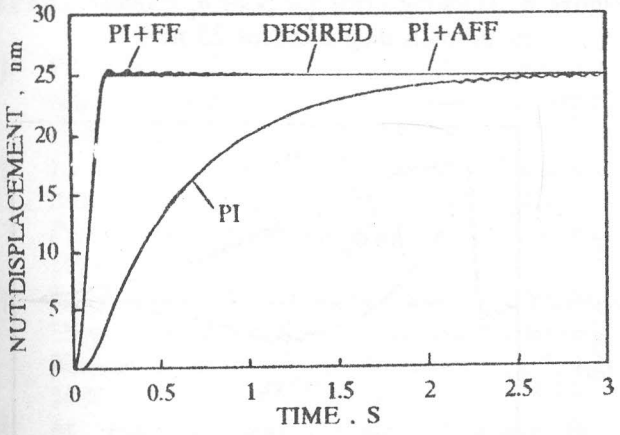

Figure 4. Plant responses to maximum desired displacement of 25 nm.

2. **Performance with non-adaptive feedforward control and PI feedback control:** The parameter adaptation algorithm (PAA) was turned off by setting the adaptation gain γ equal to zero. The values of the adaptation parameters $\hat{w}_i$ were assigned according to Eq. (14). The proportional gain K_c was increased from 125 to 1800 N.m/rad as the desired maximum nut-displacement was increased from 25 nm to 400 nm, while the integral time was kept constant at 0.05 second. The nut displacements under PI feedback control and non-adaptive feedforward control (PI+FF) are presented in Figures (4) and (5). The figures indicate that a priori knowledge of the input motion accelerates the response. The rise time was 0.1 seconds. In the region of near-zero velocity (when the maximum displacement is reached) an overshoot occurs because of the sharp turn in the trajectory. In this case, the PI+FF control compensates for more phase shift than necessary which made the plant pole faster than the modeled poles, and the actual path leads the desired path.

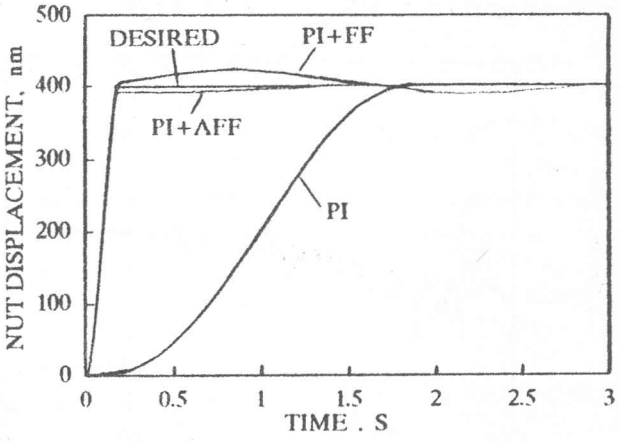

Figure 5. Plant responses to maximum desired displacement of 400 nm.

3. **Performance with adaptive feedforward control and PI feedback control (PI+AFF):** The ball screw system response was tested when the PAA was turned on. Regardless of the maximum desired nut-displacement, the controller gain and the integral time were kept at 125 N.m/rad, and 0.05 second, respectively. The system exihibts consistent behavior as shown in Figures (4) and (5). The PI+AFF scheme appears to be more robust with respect to the nonlinear dynamics than the two previous controllers. The PAA had varied the adaptation parameters in order to maintain the modelled poles as fast as the plant poles, and to minimize the tracking error.

4. Results with poor plant model: Since the ball screw torque-displacement relationship is nonlinear [8], the microdynamic spring rate is not constant. Likewise, both the values of the microdynamic displacement and the damping coefficient are uncertain because they are difficult to be measured. The ability of the controlled ball screw to track a desired trajectory in the presence of these modelling errors is vitally important. Therefore, the performance of the PI+AFF controller is evaluated when the plant model is degraded. The values of the microdynamic model K_r, θ_o, and B_r were decreased to 70 % of its original designed values. Meanwhile, K_c, τ, and the initial values of $\hat{w}_i$ were unchanged. The tracking errors due to poor model are depicted in Figures (6) to (9). The performance of the controller is not degraded when K_r is 70% of its designed value. The tracking error does not conceivably changed as shown in Figures (6) and (7).

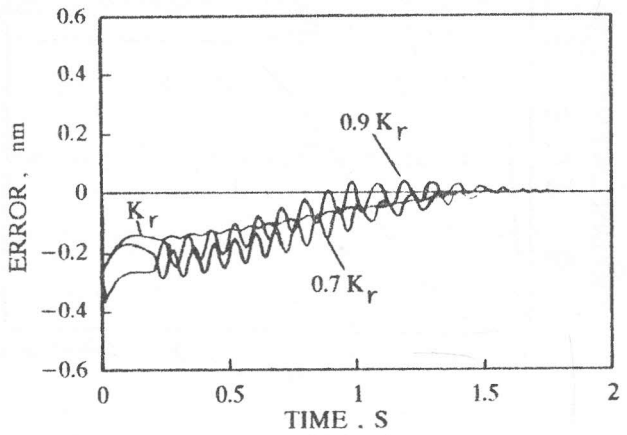

Figure 6. Tracking error for poor K_r model (maximum displacement 25 nm).

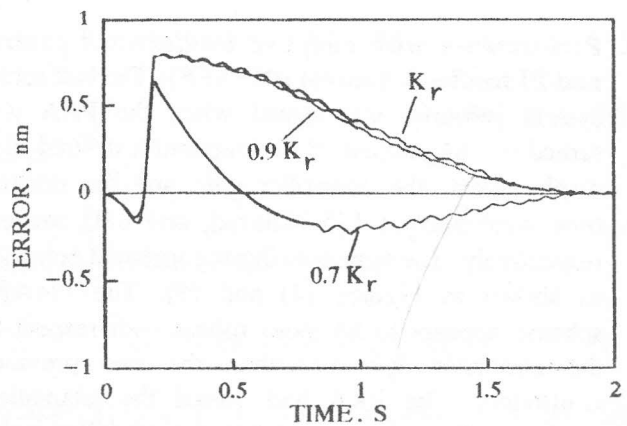

Figure 7. Tracking error for poor K_r model (maximum displacement 400 nm).

Only some oscillations with small amplitudes are noticed in the tracking error, but they are damped within a short period. Similar behavior is detected due to the decreasing of θ_o by 30% as illustrated in Figures (8) and (9). The performance of the PI+AFF controller is insensitive to the modelling error in the microdynamic damping coefficient. No significant change is observed in the tracking error as B_r was reduced by 30%.

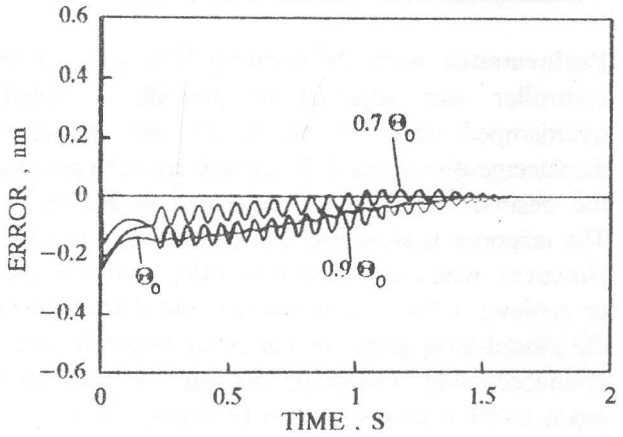

Figure 8. Tracking error for poor θ_o model (maximum displacement 25 nm).

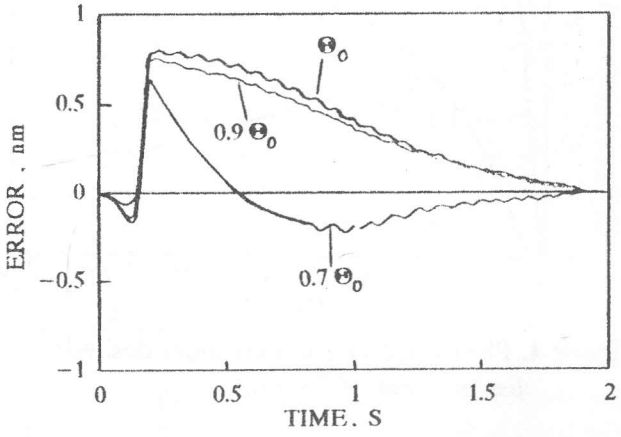

Figure 9. Tracking error for poor θ_o model (maximum displacement 400 nm).

CONCLUSIONS

The control of nonlinear dual-mode dynamics of a ball screw driven slide for nanometer positioning was

considered. The reset integrator model for slip-stick friction was implemented. The adaptive feedforward control was applied. The control system consists of a PI feedback controller, an adaptive disturbance compensator, and an adaptive feedforward controller. The stability of the control system was analyzed by Popov's theorem. The performance of the proposed control scheme was investigated and compared to the performance of both PI control, and the non-adaptive feedforward control. When the ball screw system is under PI positioning control it results in inconsistent and unpredictable responses. When a non-adaptive feedforward controller is included in the control circuit, the response is accelerated and an overshoot is observed. Both designs required delicate and continuous tuning of the PI controller in order to get full advantage of the control. On the other hand, the adaptive feedforward control is able to cope with the slip-stick effects and to produce consistent responses regardless of the desired maximum displacement and with the same PI settings. Simulation results demonstrated the effectiveness of the proposed approach in the presence of poor microdynamic model. The adaptive feedforward control has excellent robustness properties and can handle a large class of disturbances and uncertainties.

REFERENCES

[1] P.I. Ro and P.I. Hubbel, "Nonlinear Microdynamic Behavior of a Ballscrew Driven Slide " *Precision Engineering*, 1991.

[2] J.r. Cuttino and T.A. Dow, "Nanometer Actuation Using a Precision Ballscrew," *Proceedings of the ASPE Annual Conference*, 1991.

[3] S. Futami, A. Furutani and S. Yoshida, "Nanometer Positioning and its Microdynamics," *Nanotechnology*, vol. 1, No. 1, pp 31-37, July, 1990.

[4] M. Tomizuka and S.Yang, "Adaptive Pulse Width Control for Precise Positioning Under the Influence of Stiction and Coulomb Friction," *ASME J. of Dynamic Systems, Measurement, and Control*, vol. 110, pp 221-227, September, 1988.

[5] S.C. Southward et al., "Robust Nonlinear Stick-Slip Friction Compensation," *ASME J. of Dynamic Systems, Measurement, and Control*, 1990.

[6] S.P. Deweerth et al., "A Simple Neuron Servo," *IEEE Trans. on Neural Networks*, vol. 2, No. 2, pp 248-251, March, 1991.

[7] L. Guzzella and A.H. Glattfelder, "Positioning of Stick-Slip System-Comparison of a Conventional and a Variable Structure Controller Design," *Proceedings of the 1992 ACC*, pp. 1277-1281, 1992.

[8] P.I. Hubbel and P.I. Ro, "A Lyapunov Based Adaptive Control of Nonlinear Microdynamics of a Ball Screw Driven Slide For Nanometer Positioning," *Proceedings of the 1992 ACC*, pp. 201-205, 1992.

[9] M. Tomizuka, "Design of Digital Tracking Controllers for Manufacturing Applications," *ASME Manufacturing Review*, vol. 2, No. 2, pp 134-141, June, 1989.

[10] M. Tomizuka, J.S. Hu, T.C. Chiu and T.Kamano, "Synchronization of Two Motion Control Axes Under Adaptive Feedforward Control," *ASME, WAM*, Dallas, Texas, 1990.

[11] A. Smith and K.M. Lee, "An Experimental Investigation of Two Digital Tracking Controllers: Adaptive and Non-Adaptive, " *ASME, WAM, Dallas*, Texas, 1990.

[12] D. Karnopp, "Computer Simulation of Slip-Stick Friction in Mechanical Dynamic Systems," *ASME J. of Dynamic Systems, Measurement, and Control*, vol.107, pp 100-103, 1985.

[13] P.R. Dahl, "Solid Friction Damping of Mechanical Systems," *AIAA J. of Guidance, Control, and Dynamics*, vol. 14, No. 12, December, 1978.

[14] D. Haessig, and B. Friedland, "On the Modeling and Simulation of Friction," *ASME J. of Dynamic Systems, Measurement, and Control*, vol. 113, pp 354-362, September, 1991.

[15] R. Hughes, "Effects of Friction on Precision Pointing Systems," *Proceedings of the 1992 ACC*, pp 235-236, 1992.

[16] Y. Landau, *Adaptive Control: The Model Reference Approach*, Marcel Dekker, NY., 1979.

[17] R. Paden, and M.Tomizuka, "Variable Structure Discrete Time Position Control," *Proceedings of the 1993 ACC*, San Francisco, June 2-4, 1993.

[18] W. Longman, J.Juang, M.Phan and R. Ugoletti, "Automated Learning Control Through Model Updating for Precision Motion Control," *ASME Intl. ME'94 Congress & Exposition*, Chicago, November 6-11, 1994.